STM JOURNALS

Journal of
Modern Chemistry &
Chemical Technology

ISSN: 2229-6999 (Online)
ISSN: 2321-5208 (Print)
Volume 15, Issue 2, 2024
May–August
DOI (Journal): 10.37591/JoMCCT

https://journals.stmjournals.com/jomcct

Review JoMCCT

Effect of Bismuth Doping on Thiourea Crystals: A NLO Material

P. Girija[1,2]*

Abstract

Single crystals of pure and thiourea-substituted bismuth were successfully grown using the slow evaporation solution growth technique at ambient temperature. The impact of thiourea doping on the crystal properties was thoroughly investigated. Solubility tests for the grown samples were conducted at various temperatures, providing crucial data on the dissolution characteristics. Structural characterization of these crystals was performed using single crystal X-ray diffraction (XRD), confirming their crystalline nature. Energy-dispersive X-ray spectroscopy (EDS) verified the presence of bismuth in the doped bismuth thiourea crystals. The surface morphology of the crystals was examined using scanning electron microscopy (SEM), revealing detailed surface structures. Functional groups within the crystals were identified through Fourier-transform infrared (FTIR) spectroscopy, ensuring the successful incorporation of thiourea. Additionally, the non-linear optical efficiency of the doped crystals was evaluated using a modified Kurtz and Perry experimental setup, indicating an improvement due to doping. This comprehensive study highlights the potential enhancements in crystal properties and non-linear optical performance due to thiourea substitution in bismuth crystals, contributing valuable insights for future applications in optical materials and technologies.

Keywords: Non-linear optical, SEM-EDS, Powder XRD, Slow evaporation solution technique, Piezoelectric properties

INDRODUCTION

Thiourea crystals have attracted both theoretical and experimental attention because of their nonlinear optical piezoelectric properties. Thiourea possesses a large dipole moment and is a potentially useful material for frequency doubling of near-IR laser radiation. They also have a significant impact on layer technology, optical communications, and optical data storage [1–6]. The development of science in many areas has been achieved by the growth of thiourea crystals. Nonlinear optical (NLO) materials are expected to play a major role in photonic technologies, including optical information processing. Many research efforts have been undertaken to synthesize and characterize new molecules for second-order nonlinear optical (NLO) applications, such as high-speed processing, telecommunications, remote sensing lasers, and optical data storage [7–12]. Recently, the effects of the organic additives Mn(II),Ce(IV),Cs(I), Mg(I), (N_2H_4CO), (N_2 H_4CS). Organic solvents on ZTS and enhancement of SHG efficiency of thiourea on picriacid [13]. Thiourea is an interesting inorganic matrix modifier owing to its large dipole moment [14]. And its ability to form an extensive network of hydrogen bond It belongs to the orthorhombic crystal system. Only a few of thiourea complexes

***Author for Correspondence**
P. Girija
E-mail: gk-au09@yahoo.com

[1]Assistant Professor, Department of Chemistry, M.V. Muthiah Govt Arts College for Women, Dindigul, Tamil Nadu, India
[2]Assistant Professor, Department of Chemistry, Annamalai University, Annamalai Nagar, Chidambaram, Tamil Nadu, India

Received Date: February 12, 2024
Accepted Date: May 04, 2024
Published Date: July 30, 2024

Citation: P. Girija. Effect of Bismuth Doping on Thiourea Crystals: A NLO Material. Journal of Modern Chemistry & Chemical Technology. 2024; 15(2): 10–16p.

viz, Zinc thiourea sulphate [15, 16], Cadmium thiourea acetate[17], bis thiourea cadmium chloride. The search for new and efficient NLO materials has resulted in the development of a new class of materials called organic mixed crystals, In this paper, bismuth doped thiourea crystal is synthesized and grow by slow evaporation technique at ambient temperature.

EXPERIMENTAL

Bismuth-doped thiourea crystals were grown using a slow-evaporation technique at ambient temperature. Thiourea (2 g) and 2.6 g of bismuth (AR Merck grade) were dissolved in triple distilled water. The mixture was stirred for three hours and filtered to remove suspended particles. The solution was maintained under ambient conditions. In the solution growth technique, the crystal size depends on the amount of material available in the solution, which in turn is determined by the solubility of the material in the solvent. Images of the as-grown doped and undoped crystals are shown in Figures 1(a) and (b). The surface morphology was observed using a JEOL JSM 5610 LV scanning electron microscope (SEM). It has a resolution of 3.0 Â nm and an acceleration voltage of 0.3 to 30 kV, with a maximum magnification of 2,00,000 times. Energy dispersive X-ray spectroscopy (EDS) chemical microanalysis was performed in conjunction with SEM. The EDS X-ray detector measured the number of emitted X-ray photons and their energies. Single-crystal X-ray diffraction (XRD) studies were carried out using a Bruker AXS (Kappa APEX II) X-ray diffractometer. Data were collected using a diffraction system that employs graphite-monochromated Mo Kα radiation (λ = 0.71073 Å). Fourier-transform infrared spectroscopy (FTIR) studies were carried out on the grown crystals to understand their structure and bonding. The FTIR spectrum of bismuth-doped thiourea crystals was recorded on an AVATAR 330 spectrometer using the KBR pellet technique in the wavelength range 400-4000cm^{-1}. The powder XRD patterns of the grown crystals were recorded using Cu Kα radiation (1.54060 Å). The nonlinear property of the bismuth-doped thiourea crystal was confirmed by shining a Nd: YAG laser (λ=1046 nm) on the plate of the grown crystal.

RESULTS AND DISCUSSION

Scanning Electron Microscope with Energy Dispersive Spectroscopy (EDS)

[SEM study JEOL JSM 5610lv] provides information about the surface nature and its suitability for device fabrication and is also used to check the presence of imperfections. The effectiveness of the different impurities in changing the surface morphology was different has been reported. Figure 2 shows the surface morphology of bismuth-doped thiourea crystals. The micrograph shows a larger scattered center due to the heavy doping of bismuth in the thiourea crystal matrix. Micrograph (a) depicts the surface features of the undoped specimen and shows a reasonably good uniform surface with some roughness, which could be due to impurities. Micrograph (b) depicts the surface features of the as-grown (bismuth-doped thiourea) specimen and shows some bubble voids, which could be quite likely due to the evaporation of the solvent from the crystal surface. The doping of bismuth, which results in its incorporation into the crystal, is also non-uniform.

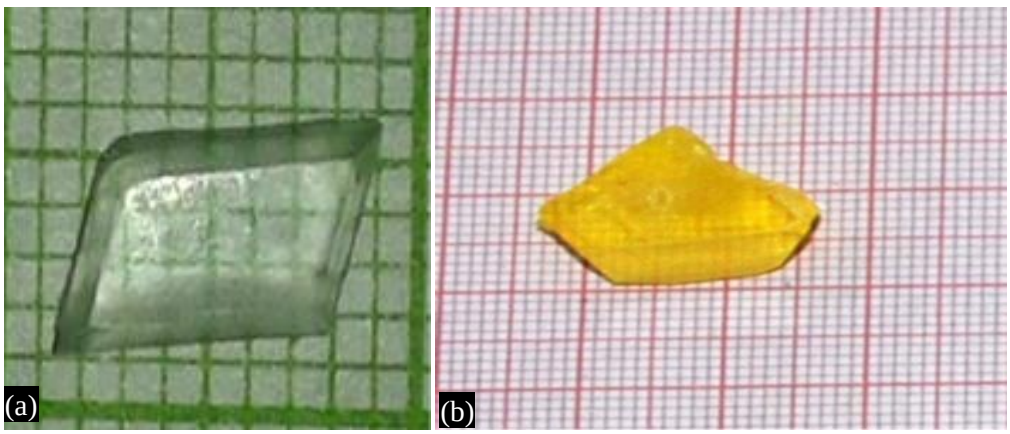

Figure 1. (a) Pure thiourea (b) bismuth doped thiourea.

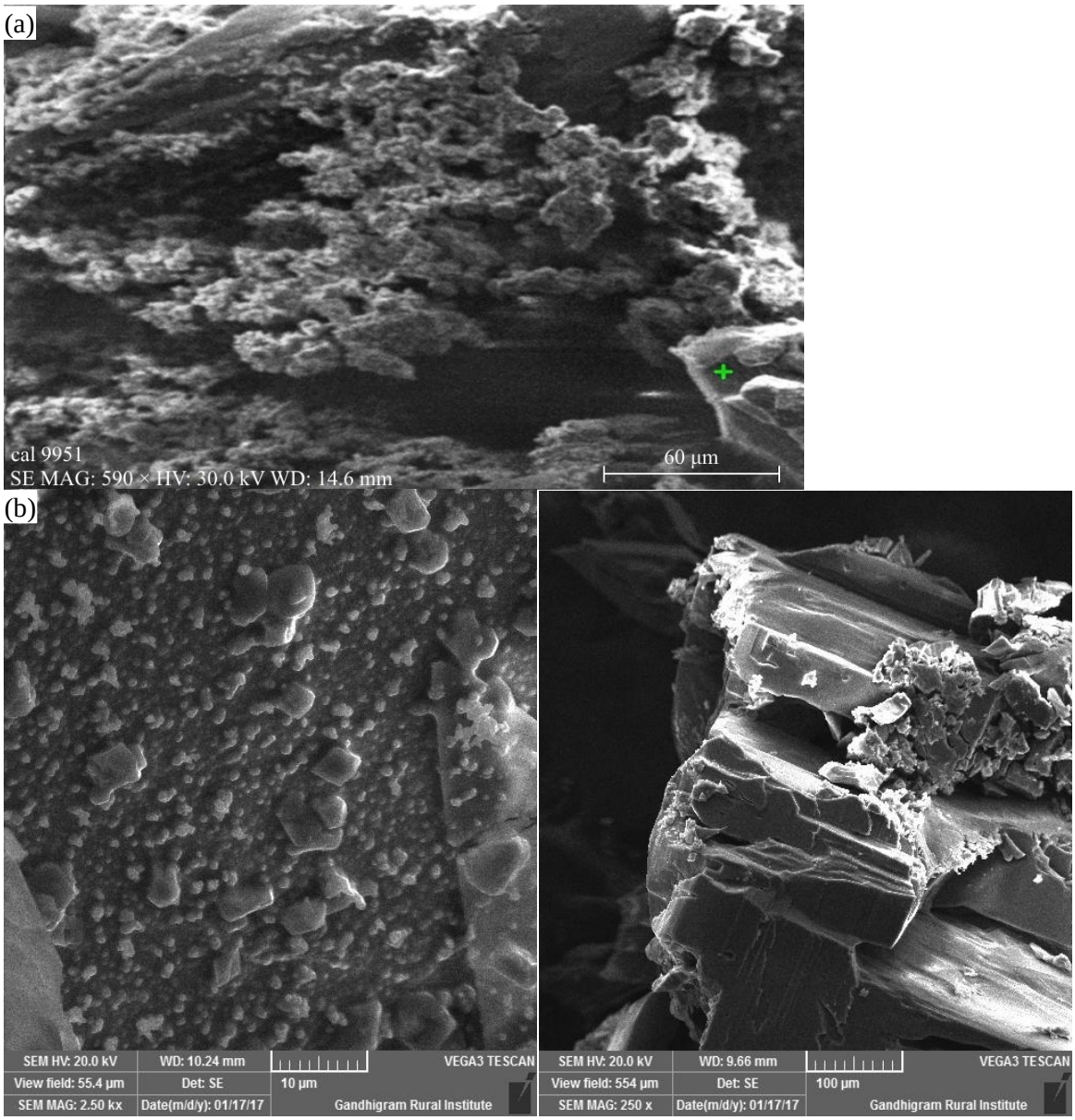

Figure 2. SEM incorporation (a) pure thiourea (b) bismuth doped thiourea crystals.

The EDS graph confirms the presence of bismuth in the crystalline matrix (Figure 3). Analysis of the surface at different sites showed that only a small quantity of dopant was incorporated into the thiourea crystalline matrix, which was non uniform over the surface connected to the adsorption mechanism.

Single Crystal XRD Analysis

Single crystal X-ray diffraction (XRD) studies were conducted using a Bruker AXS (Kappa APEX II) X-ray diffractometer to determine the lattice parameters of the pure thiourea crystals. The lattice parameters for pure thiourea were found to be: a=5.53A˚a = 5.53 \text{Å}a=5.53A˚, b=7.73A˚b = 7.73 \text{Å}b=7.73A˚, and c=8.62A˚c = 8.62 \text{Å}c=8.62A˚, with α=β=γ=90∘\alpha = \beta = \gamma = 90^\circα=β=γ=90∘ and a cell volume of 368.0A˚3368.0 \text{Å}^3368.0A˚3. These parameters indicate that the crystal had an orthorhombic structure.

Upon doping with Bi, a slight variation in the cell parameter values was observed. These variations are indicative of lattice strain introduced by the incorporation of Bi into the thiourea crystal matrix. The lattice parameters of bismuth-doped thiourea are listed as follows (Table 1).

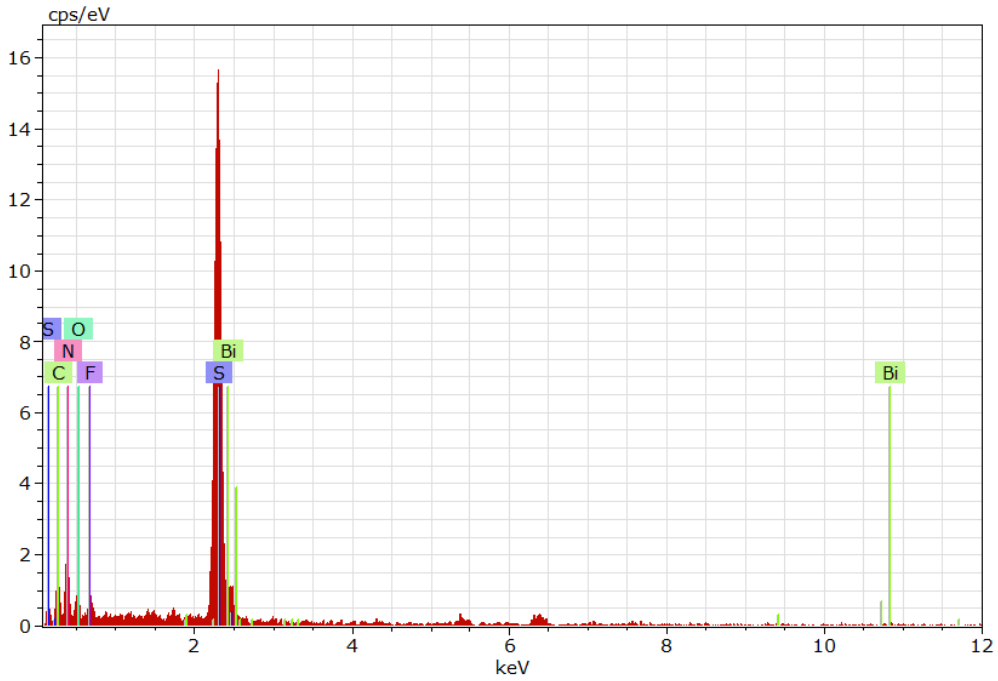

Figure 3. EDS graph of Bismuth doped thiourea crystal**.**

Table 1. Cell parameters values of pure and Bismuth doped thiourea crystals.

Crystals	a_A^0	b_A^0	c_A^0	V_A^{03}	System
Thiourea	5.53	7.73	8.62	368	Orthorhombic
Bi/Thiourea	5.535	7.667	8.621	368.0	Orthorhombic

These slight differences in the lattice parameters confirmed the successful doping of Bi into the thiourea crystals, causing minor adjustments in the crystal structure. The orthorhombic nature of the crystal was preserved, but the introduction of bismuth led to observable changes in the unit cell dimensions, reflecting the impact of the dopant on the crystal lattice. The slight difference in the cell parameter values could be attributed to the doping of bismuth metal into thiourea.

Powder X-ray Diffraction

The powder XRD patterns of pure and bismuth-doped thiourea are shown in Figure 4. Powder X-ray diffraction analysis was performed using graphite-monochromated Cuk_α radiation. The powder x-ray diffraction patterns of the pure and bismuth-doped thiourea crystals are shown in to pure thiourea, the intensity of the doped crystals is reduced, which is due to the small particle size. The particle size can be calculated using the Scherrer equation, which is 16 nm for bismuth-doped thiourea crystals as

$$t = K\lambda/(\beta \cos\theta)$$

Where;
t- averaged dimension of crystallities
K- is the scherrer constant,
λ is the wavelength of the X-ray;
θ-peak position measured during radiation
β is the integral breadth of reflection (in radian2θ) located at 2θ.

Fourier Transform Infrared Spectroscopy

FTIR spectra are recorded for pure and doped thiourea crystals by using AVATAR 330 FT-IR instrument by KBr pellet technique in the range 400–4000 cm^{-1} the Figure 5 shows the FTIR spectra of thiourea and Bismuth doped thiourea crystal investigation the presence of functional groups and their

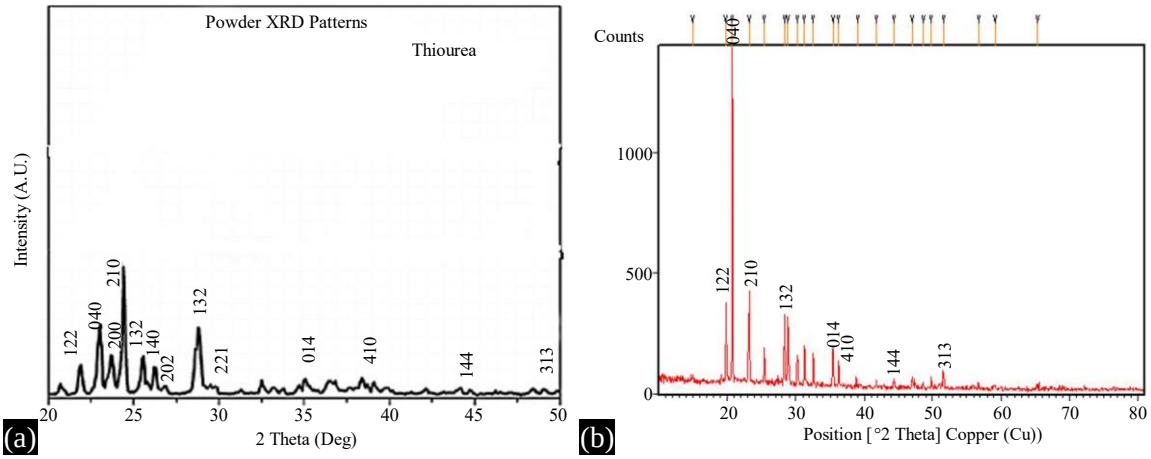

Figure 4. Powder XRD patterns of (a) pure thiourea (b) bismuth doped thiourea crystal.

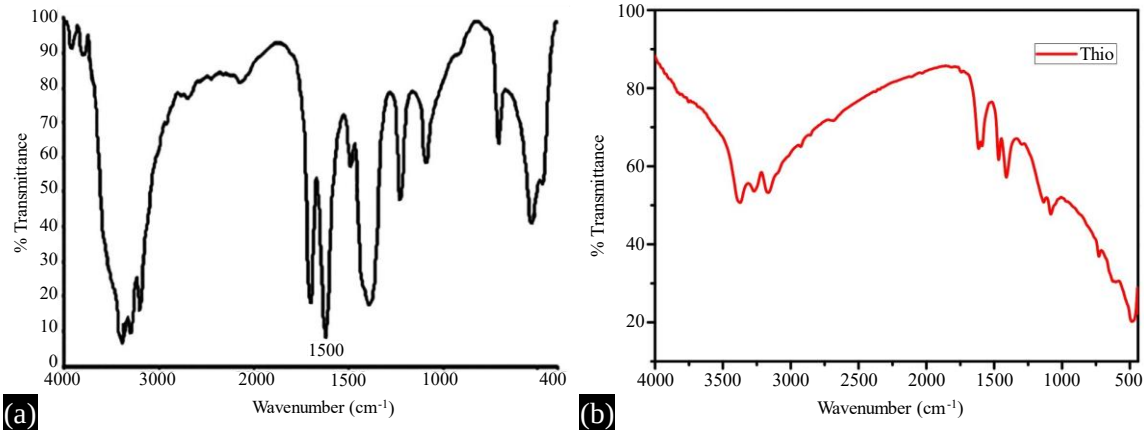

Figure 5. FTIR Spectra of (a) pure thiourea, (b) FTIR of bismuth doped thiourea crystal.

Table 2. Comparison of vibrational frequencies of pure and Bismuth doped thiourea crystal.

Wavelength of thiourea cm^{-1}	Wavelength of Bi|Thiourea cm^{-1}	Tentative assignment
3395	3373.85	$\gamma_{as}(NH_2)$
3179	3167.51	$\gamma_s(NH)$
2674	2685.39	$\gamma_s(NH_2$
2104	2031.64	γ (NCN), NH_3^+
1621	1615.09	$\delta(NH_2)$
1464	1467.56	$\gamma_{as(CN)}$
1395	1410.67	$\gamma_{as(C=S)}$
1089	1082.83	$\gamma_{s(CN)}$
729	729.99	$\gamma_s(C=S)$
485	485	$\delta_{as(NCN)}$

vibrational modes between 400 and 4000 cm^{-1}. The shifts in the vibrational frequencies of the doped specimen compared to those of pure thiourea are tabulated as follows. A comparison of the characteristic frequencies of the thiourea and bismuth-doped thiourea crystals is shown in Table 2.

In the analysis, a very slight shift in some characteristic vibrational frequencies of pure thiourea was observed due to bismuth doping, likely caused by lattice strain development. Specifically, the

wavenumber for the asymmetric NH_2 absorption band in thiourea, originally at 3395 cm^{-1}, shifted to 3373.85 cm^{-1} in bismuth-doped thiourea crystals. This shift, along with the broadening of the band in the doped crystals compared to that of pure thiourea, suggests the absence of strong hydrogen bonding in the doped specimens. Instead, a weaker tendency to form hydrogen bonds was observed.

Additionally, the bonding vibrations (δ as NH_2, γC=S) of thiourea at 1621 cm^{-1} and 1395 cm^{-1} shifted to 1651.9 cm^{-1} and 1410.67 cm^{-1}, respectively, in the doped specimens. These shifts indicate the formation of a bismuth-thiourea mixed crystal. The changes in vibrational frequencies and band broadening provided evidence of the interaction between bismuth and thiourea, resulting in altered bonding characteristics and the formation of a mixed crystal structure. This insight into the vibrational properties underscores the impact of Bi doping on the structural and bonding dynamics within the thiourea crystal matrix.

CONCLUSION

After careful optimization, single crystals of undoped and bismuth-doped thiourea were synthesized using a slow evaporation solution growth technique with water as the solvent at ambient temperature. X-ray diffraction (XRD) analysis confirmed the improvement in crystalline quality of the grown thiourea crystals with the presence of bismuth as a dopant, slightly altering the lattice parameter values. Fourier-transform infrared (FTIR) spectroscopy validated the presence of various functional groups in the molecule, indicating that the doping process maintained the chemical integrity of the thiourea crystals.

Scanning electron microscopy (SEM) revealed significant surface changes in the bismuth-doped specimens, characterized by large scattered centers in their morphology. This morphological variation suggests that the dopant affected the crystal surface structure. Energy-dispersive X-ray spectroscopy (EDS) further confirmed the presence of bismuth within the thiourea crystal matrix, providing direct evidence of successful doping.

These comprehensive characterizations demonstrate that bismuth doping improves the crystalline quality and alters the structural properties of the thiourea crystals, potentially enhancing their optical and electronic properties. These findings suggest that bismuth-doped thiourea crystals could be valuable for various applications that require modified material properties.

REFERENCES

1. Madhurambal G, Mariappan M. Growth and characterization of urea-thiourea non-linear optical organic mixed crystal. Indian J Pure Appl Phys. 2010;48(4):264-270.
2. Madhurambal G, Mariappan M, Mojumdar SC. TG–DTA, UV and FTIR spectroscopic studies of urea–thiourea mixed crystal. J Therm Anal Calorim. 2010;100(3):853-6. doi: 10.1007/s10973-010-0763-3.
3. Ravindran B, Madhurambal G, Mariappan M, Mojumdar SC. Synthesis and characterization of some single crystals of thiourea urea zinc chloride. J Therm Anal Calorim. 2011;104(3):893-9. doi: 10.1007/s10973-011-1291-5.
4. Das M, Prasad R, Sent P. Structural analysis and second-order non-linear optical activity of urea hydrogen peroxide adduct. Indian J Pure Appl Phys. 2006;44(7):554-8.
5. Ravindran B, Madhurambal G, Mariappan M, Ramamurthi K, Mojumdar SC. Growth and characterization of mercury cinnamate single crystal. J Therm Anal Calorim. 2011;104(3):909-14. doi: 10.1007/s10973-011-1292-4.
6. Mariappan M, Madhurambal G, Ravindran B, Mojumdar SC. Thermal, FTIR and microhardness studies of bisthiourea-urea single crystal. J Therm Anal Calorim. 2011;104(3):915-21. doi: 10.1007/s10973-011-1293-3.
7. Waghuley SA, Yenorkar SM, Yawale SS, Yawale SP. Application of chemically synthesized conducting polymer-polypyrrole as a carbon dioxide gas sensor. Sens Actuators B Chem. 2008;128(2):366-73. doi: 10.1016/j.snb.2007.06.023.

8. Gunasekaran S, Anand G, Arun Balaji R, Dhanalakshmi J, Kumaresan S. Crystal growth and comparison of vibrational and thermal properties of semi-organic nonlinear optical materials. Pramana. 2010;75:683–690.
9. Jayarama A, Dharmaprakash SM. Crystal growth and characterization of thiourea mixed ammonium dihydrogen phosphate. Indian J Pure Appl Phys. 2006;44(6):455-60.
10. Ogura K, Shiigi H. A CO[sub 2] sensing composite film consisting of base-type polyaniline and poly(vinyl alcohol). Electrochem Solid-State Lett. 1999;2(8):478. doi: 10.1149/1.1390876.
11. Maier J, Holzinger M, Sitte W. Fast potentiometric CO2 sensors with open reference electrodes. Solid State Ionics. 1994;74(1-2):5-9. doi: 10.1016/0167-2738(94)90430-8.
12. Marotta A, Buri A. Kinetics of devitrification and differential thermal analysis. Thermochim Acta. 1978;25(2):155-60. doi: 10.1016/0040-6031(78)85003-5.
13. Okaya Y. The crystal structure of potassium acid phthalate, KC6H4COOH.COO. Acta Crystallogr. 1965;19(6):879-82. doi: 10.1107/S0365110X65004590.
14. Ram S. Observation of enhanced dielectric permittivity in Bi3+ doped BaFe12O19 ferrite. J Magn Magn Mater. 1989;80(2-3):241-5. doi: 10.1016/0304-8853(89)90124-8.
15. Singh P, Babbar VK, Razdan A, Srivastava SL, Agrawal VK, Goel TC. Dielectric constant, magnetic permeability and microwave absorption studies of hot-pressed Ba-CoTi hexaferrite composites in X-band. J Mater Sci. 2006;41(24):7190-6. doi: 10.1007/s10853-006-0921-y.
16. Wu HB, Chen Y, Wu MY, Guan CR, Yu XY. 3d measurement technology by structured light using stripe-edge-based gray code. InJournal of Physics: Conference Series 2006 Oct 1 (Vol. 48, No. 1, p. 537). IOP Publishing.
17. An SY, Lee SW, Shim IB, Kim CS. Magnetic properties of water-based sol-gel derived BaFe12O19/SiO2/Si(100) thin films. IEEE Trans Magn. 2001;37(4):2585-8. doi: 10.1109/20.951243.

